



Single Cell and Spatial Technologies to Advance Your Research

Resolve highly complex biological systems, while bringing into focus the details that matter most. Explore biology at true resolution.

Join the conversation with exclusive live talks at Europe-friendly times, or enjoy on-demand recordings at your leisure!

[Join the Conversation](#)

Together we succeed!

Get a sneak peek into the progress we're making as a community to optimize single cell and spatial transcriptomics workflows at every step.

10x Genomics & Illumina Coffee-Break Conversations

Learn how single cell sequencing and spatial transcriptomics can unlock biological mysteries across a number of research areas.

10x Genomics European Virtual Scientific Symposium


Learn how single cell and spatial technologies are driving fundamental discoveries across multiple areas of biology, including cancer, immunology, neuroscience—and COVID-19.

And more...



ARTICLE

Partial T cell defects and expanded CD56^{bright} NK cells in an SCID patient carrying hypomorphic mutation in the *IL2RG* gene

Cristina Cifaldi¹ | Nicola Cotugno^{2,3} | Silvia Di Cesare^{1,3} | Silvia Giliani⁴ | Gigliola Di Matteo^{1,3} | Donato Amodio^{1,3} | Eva Piano Mortari⁵ | Maria Chiriaco¹ | Danilo Buonsenso⁶ | Paola Zangari¹ | Daria Pagliara⁷ | Stefania Gaspari⁷ | Rita Carsetti⁵ | Paolo Palma^{2,3} | Andrea Finocchi^{1,3} | Franco Locatelli^{7,8} | Paolo Rossi^{1,2,3} | Margherita Doria²  | Caterina Cancrini^{1,3}

¹Unit of Immune and Infectious Diseases, Academic Department of Pediatrics, Bambino Gesù Childrens' Hospital-Scientific Institute for Research and Healthcare (IRCCS), Rome, Italy

²Research Unit of Congenital and Perinatal Infection, Academic Department of Pediatrics, Bambino Gesù Childrens' Hospital-Scientific Institute for Research and Healthcare (IRCCS), Rome, Italy

³Department of Systems Medicine, University of Rome Tor Vergata, Rome, Italy

⁴Department of Molecular and Translational Medicine, A. Nocielli Institute for Molecular Medicine, University of Brescia, Brescia, Italy

⁵Immunology Research Division, Bambino Gesù Childrens' Hospital IRCCS, Rome, Italy

⁶Department of Woman and Child Health and Public Health, Fondazione Policlinico Universitario A. Gemelli, IRCCS, Rome, Italy

⁷Department of Pediatric Hematology and Oncology, Bambino Gesù Childrens' Hospital IRCCS, Rome, Italy

⁸Department of Pediatrics, Sapienza University of Rome, Rome, Italy

Correspondence

Caterina Cancrini, Bambino Gesù Childrens' Hospital, Piazza S. Onofrio 4, 00165, University of Rome Tor Vergata, Via Montpellier 1, 00133, Rome, Italy.

Email: cancrini@med.uniroma2.it

Margherita Doria (lead author), Bambino Gesù Childrens' Hospital, Piazza S. Onofrio 4, 00165, Rome, Italy.

Email: doria@uniroma2.it

Abstract

X-linked severe combined immunodeficiency (X-SCID) caused by full mutation of the *IL2RG* gene leads to T⁻ B⁺ NK⁻ phenotype and is usually associated with severe opportunistic infections, diarrhea, and failure to thrive. When *IL2RG* hypomorphic mutation occurs, diagnosis could be delayed and challenging since only moderate reduction of T and NK cells may be present. Here, we explored phenotypic insights and the impact of the p.R222C hypomorphic mutation (*IL2RG*^{R222C}) in distinct cell subsets in an 8-month-old patient with atypical X-SCID. We found reduced CD4⁺ T cell counts, a decreased frequency of naïve CD4⁺ and CD8⁺ T cells, and an expansion of B cells. Ex vivo STAT5 phosphorylation was impaired in CD4⁺CD45RO⁺ T cells, yet compensated by supra-physiological doses of IL-2. Sanger sequencing on purified cell subsets showed a partial reversion of the mutation in total CD3⁺ cells, specifically in recent thymic emigrants (RTE), effector memory (EM), and CD45RA⁺ terminally differentiated EM (EMRA) CD4⁺ T cells. Of note, patient's NK cells had a normal frequency compared to age-matched healthy subjects, but displayed an expansion of CD56^{bright} cells with higher perforin content and cytotoxic potential, associated with accumulation of NK-cell stimulatory cytokines (IL-2, IL-7, IL-15). Overall, this report highlights an alteration in the NK-cell compartment that, together with the high disease-phenotype variability, should be considered in the suspicion of X-SCID with hypomorphic *IL2RG* mutation.

KEYWORDS

common gamma chain, cytokine signaling, primary immune deficiency

Abbreviations: CMV, cytomegalovirus; CT, computed tomography; GI, gastro-intestinal tract; HSCT, hematopoietic stem cell transplantation; IGV, integrative genomics viewer; IL-2R, IL-2 receptor; NGS, next generation sequencing; PID, primary immune deficiency; RTE, recent thymic emigrants; SCID, severe combined immune deficiency; Tfh, follicular helper T cell; TRECs, T-cell receptor excision circle; Treg, regulatory T cell; WBC, white blood cell; X-SCID, X-linked severe combined immunodeficiency.

Received: 8 November 2019 | Revised: 3 February 2020 | Accepted: 19 February 2020

J Leukoc Biol. 2020;108:739–748.

www.jleukbio.org

©2020 Society for Leukocyte Biology

739

1 | INTRODUCTION

The γ -chain (γ_c) encoded by the *IL2RG* gene is a key subunit shared by different cytokine receptor complexes binding to IL-2, IL-4, IL-7, IL-9, IL-15, and IL-21, which play key roles in T, B, and NK cell development and function.¹ The binding of IL-2 to its receptor (IL-2R) leads to JAK1- and JAK3-mediated activation of STAT5, a key step of cytokine signaling.^{2,3} Null variants of the *IL2RG* gene lead in humans to typical X-linked severe combined immune deficiency (X-SCID) (OMIM 300400) presenting with abnormal T cell development and function, absence of NK cells, and normal frequency of defective B cells.⁴⁻⁶ In these patients, the absence of IL-2, IL-7, IL-15, and IL-21 signaling impedes T and NK cell development, the most prominent immunological abnormalities. Affected patients usually present disease onset in early infancy, with severe combined infections, chronic diarrhea, and failure to thrive, often leading to fatality within the first year of life.⁷ The most frequently adopted curative solution is represented by the allogeneic hematopoietic stem cell transplantation (HSCT), which showed a better outcome when neonatal diagnosis was available due to routine newborn screening.⁸ Besides, gene therapy was tested in clinical trials on patients affected by X-SCID showing encouraging clinical efficacy and safety profile.⁹⁻¹¹ When hypomorphic *IL2RG*^{R222C} mutation of the γ_c subunit occurs, a less severe and more variable clinical history makes diagnosis challenging and often delayed. The *IL2RG*^{R222C} mutation leads to an atypical and highly variable immune phenotype ranging from normal to moderately reduced T and NK cell frequency and function.¹²⁻¹⁴ In rare cases, first described by Stephan et al. in 1996, *IL2RG*-mutated patients had spontaneous mutation reversion leading to partial disease correction.¹⁵ However, only few studies have investigated whether a differential mutation reversion within lymphocyte subsets can lead to diverse functional and clinical presentations.¹⁶

Here, we report a detailed analysis of T, B, and NK cell frequency and function in an 8-month-old boy diagnosed with atypical X-SCID due to a c.C664T p.R222C mutation. A full characterization of mutation reversion within purified subsets and the possible impact on lymphocyte function is presented.

2 | MATERIALS AND METHODS

2.1 | Patient

Clinical data and DNA specimens from the subject were collected following procedures in accordance with the ethical standards of the 1964 Helsinki declaration and its later amendments. Parents of the patient provided informed consent for genetic studies and publication.

2.2 | Cells

PBMCs and K562 cells were cultivated in RPMI 1640 medium supplemented with 10% FBS, 0.2 mM L-glutamine, and 100 units/ml penicillin-streptomycin (Euroclone).

2.3 | T and B cell immunophenotype

Flow cytometry analyses were performed on EDTA blood samples within 24 h of venipuncture. Full list of previously titrated Abs is available in Extended Methods. Data were acquired on a FACSCanto II (Becton Dickinson) and analyzed by FlowJo software 9.3.2 (Tree Star Inc.).

2.4 | NK cell immunophenotype

PBMCs and serum were obtained by Ficoll separation and cryopreserved until use. The immunolabeling procedure and Abs are described in Extended Methods. Data were acquired on a FACSCanto II (BD Biosciences) or Cytoflex (Beckman Coulter) and analyzed by FlowJo (TreeStar) or Kaluza (Beckman Coulter).

2.5 | NK cell functional assays

Flow cytometry-based cytotoxicity assays were performed using PBMCs as effectors (E) and K562 cells as targets (T). IFN- γ production was measured in cytokine-stimulated and in not stimulated NK cells. Full procedures are described in Extended Methods.

2.6 | Detection of cytokines

The concentration of IL-2, IL-7, and IL-15 in plasma samples was measured in duplicates by xMAP Technology on a LX200 Luminex instrument by Labospace s.r.l. (Milano, Italy) service provider.

2.7 | Cell sorting

Cryopreserved PBMC were thawed and stained with Abs and Vivid (Pacific Blue) for viability testing. Viable cells were sorted by FACS Ari-III (BD Biosciences) setting on the stringent 4-Way purity precision mode. Due to the paucity of cells recovered from the patient, the purity of sorted cells was checked on distinct cell samples processed with the same sorting strategy, showing a >95% purity by FACS analysis (data not shown). DNA was isolated from sorted cells with Qiagen kit according to manufacturer's instruction and stored at -20°C till analysis.

2.8 | Ion torrent gene target library preparation, next generation sequencing, and bioinformatics analysis

Five nanograms of genomic DNA (gDNA) were used for library preparation according to standard protocols. Ampliseq Design Samples were processed and analyzed as previously described.¹⁷

2.9 | Sanger sequencing

gDNA was isolated from total PBMCs. The coding exons of the *IL2RG* gene (NCBI NM_000206) were amplified by PCR (GoTaq Polymerase-Promega), sequenced using the BigDye Terminator version 3.1 Cycle Sequencing Kit (Applied Biosystems, Foster City, CA) and analyzed on an ABI PRISM 3130 and 310 automated sequencers (Applied Biosystems, Foster City, CA).

TABLE 1 Haematological and Immunological profile

	Gated on	Pt (8 m)	Normal range (5–9 m)	Pt (128 days after HSCT)
WBC 10 ³ /uL	-	11.02	6.00–17.00 ^a	3.34
Hemoglobin g/dL	-	10.1	10.50–15.50 ^a	11.4
Total Lymphocyte count 10 ³ /uL	-	5.85	3.00–11.22 ^a	1.77
Eosinophils 10 ³ /uL	-	1.90	0–1.90 ^a	0.21
% (10 ³ cells/uL) Lymphocyte subsets				
CD3 ⁺ CD45 ⁺	Lymphocytes	45.5 (2.66)	49.0–95.0 ^b (1.4–11.5) ^b	62
CD3 ⁻ CD16 ⁺ CD56 ⁺	Lymphocytes	11.3 (0.66)	2.0–36.0 ^b (1.0–11.5) ^b	12.46
CD3 ⁺ CD4 ⁺	Lymphocytes	10.4 (0.60)	27.0–81.0 ^b (1.0–7.2) ^b	29.3
CD3 ⁺ CD8 ⁺	Lymphocytes	36.7 (2.14)	10.0–35.0 ^b (0.2–5.4) ^b	23.40
CD19 ⁺ CD45 ⁺	Lymphocytes	41.9 (2.45)	12.4–33.6 ^c (0.5–2.1) ^c	20
% CD3 lymphocyte subsets				
TCR α/β ⁺	CD3 ⁺	93.8	39–94 ^b	-
TCR γ/δ ⁺	CD3 ⁺	3.1	0.82–10 ^b	-
CD4 ⁻ CD8 ⁻	TCR α/β ⁺	0.1	0.39–4 ^b	-
% CD4 lymphocyte subsets				
CD27 ⁺ CD45RA ⁺ Naïve	CD4 ⁺	11.5	77.0–97.0 ^b	-
CD31 ⁺ CD45RA ⁺ (Recent Thymic Emigrants, RTE)	CD4 ⁺	9.83	65.0–90.0 ^b	-
CD27 ⁺ CD45RA ⁻ (Central Memory)	CD4 ⁺	86	2.0–59.0 ^b	-
CD27 ⁻ CD45RA ⁻ (Effector Memory)	CD4 ⁺	1.65	0.07–1.0 ^b	-
CD27 ⁻ CD45RA ⁺ (Effector Memory CD45RA ⁺ , EMRA)	CD4 ⁺	0.83	0.00033–7.3 ^b	-
CD25 ⁺ CD127 ^{low} FOXP3 ⁺ (Regulatory T cell, Treg)	CD4 ⁺	1.31	4.86–7.09 ^a	-
CD45RO ⁺ CXCR5 ⁺ (Follicular helper T cell, Tfh)	CD4 ⁺	13.2	2.3–7.4 ^a	-
% CD8 lymphocyte subsets				
CCR7 ⁺ CD45RA ⁺ (Naïve)	CD8 ⁺	1.04	31.0–100 ^b	-
CCR7 ⁺ CD45RA ⁻ (Central Memory)	CD8 ⁺	0.88	0.1–13.0 ^b	-
CCR7 ⁻ CD45RA ⁻ (Effector Memory)	CD8 ⁺	47.3	1.0–100 ^b	-
CCR7 ⁻ CD45RA ⁺ (Effector Memory CD45RA ⁺ , EMRA)	CD8 ⁺	50.8	5.0–78.0 ^b	-
% B lymphocyte subsets				
CD27 ⁺ IgD ⁺ IgM ⁺ (Unswitched memory)	CD19 ⁺	1.13	2.4–9.9 ^c	-
CD27 ⁺ IgD ⁻ IgM ⁻ (Switched memory)	CD19 ⁺	0.05	0.6–3.7 ^c	-
CD27 ⁻ IgD ⁺ IgM ⁺ (Naïve)	CD19 ⁺	98.1	87.3–95.1 ^c	-
CD27 ⁻ IgD ⁻ IgM ⁻	CD19 ⁺	0.67	0.4–2.7 ^c	-
CD21 ^{low} CD38 ^{low}	CD19 ⁺	0.33	0.5–33.0 ^d	-
CD24 ⁺⁺ CD38 ⁺⁺ (Transitional)	CD19 ⁺	3.6	5.0–50.0 ^d	-
CD19 ⁺ CD27 ⁺ (Memory)	CD19 ⁺	1.09	3.5–12.2 ^c	-
% NK cell subsets				
CD56 ^{bright}	NK	33.09	14.14–17.85 ^e	-
CD56 ^{dim}	NK	52.79	59.11–70.05 ^e	-
CD56 ^{neg}	NK	12.96	13.77–25.40 ^e	-
CD56 ^{bright} NKG2A ⁺ NKG2C ⁻ CD57 ⁻	NK	32.86	9.5–11.30 ^e	-
NKG2D ⁺	NK	91.46	38.25–41.14 ^e	-
Perforin ⁺	NK	99.63	92.41–96.40 ^e	-
DNAM1 ⁺	NK	90.25	37.34–49.53 ^e	-
NKp46 ⁺	NK	89.83	60.61–77.22 ^e	-
KIR ⁺	NK	49.74	39.40–56.85 ^e	-

(Continued on next page)

TABLE 1 (Continued)

	Gated on	Pt (8 m)	Normal range (5–9 m)	Pt (128 days after HSCT)
NKG2A ⁺	NK	49.15	54.68–72.05 ^e	–
NKG2C ⁺	NK	41.88	4.82–21.27 ^e	–
NKG2A ⁺ KIR [–] CD57 [–] (early differentiated)	CD56 ^{dim}	23.31	52.56–56.42 ^e	–
NKG2A [–] KIR ⁺ CD57 ⁺ (mature)	CD56 ^{dim}	37.91	3.96–17.26 ^e	–
NKG2A [–] KIR ⁺ CD57 ⁺ NKG2C ⁺ (memory-like)	CD56 ^{dim}	33.81	1.85–2.72 ^e	–
Serum immunoglobulin levels				
IgG (mg/dl)		84	360–1180 ^a	–
IgA (mg/dl)		9	36–165 ^a	–
IgM (mg/dl)		10	35–104 ^a	–
IgE (kU/l)		42.9	<13.0 ^a	–
T cell proliferation (PI)				
PHA		35	31–317 ^a	
OKT3		13	27–136 ^a	
Ig secretion by CpG-stimulated B cells ^f				
IgG (μg/ml)		0	0.04–10 ^a	
IgA		0	0.05–8 ^a	
IgM		2.4	1.3–23 ^a	

m, months. TCR, T cell receptor. WBC, white blood cell. PI, proliferation index (counts stimulated/unstimulated).

^aInternal laboratory values.

^bNormal tolerance interval for age reported in supplementary reference.³¹

^cNormal range for age.³²

^dNormal tolerance interval for age.³³

^eNormal values are presented as value range of three age-matched healthy donors.

^fThe assay was performed as previously described.³⁴

2.10 | STAT5 phosphoflow analysis

After overnight serum-starvation, PBMCs were stimulated with 10, 100, and 1000 IU/ml of IL-2 (PeproTech, NJ, USA) for 10 min at 37°C, stained with anti-pSTAT5 Ab, and analyzed by FACScanto II flow cytometer (BD Biosciences) to measure STAT5 phosphorylation. Detailed procedure is available in Extended Methods.

3 | RESULTS AND DISCUSSION

An 8-month-old male, only child born from non-consanguineous Caucasian parents, was transferred to our hospital for suspected primary immune deficiency (PID). His clinical record was characterized by atopic dermatitis and milk protein allergy from the third month of life. At the age of 7 months, he was admitted to another hospital for interstitial pneumonia, failure to thrive, malabsorption, mild anemia, and a postnatal cytomegalovirus (CMV) infection. Chest computed tomography (CT) showed “ground glass” areas associated to pseudonodular areas. CT scan and abdomen sonography showed respectively a small thymus (26 × 9 × 14 mm) and mild hepatosplenomegaly. When the present study was performed (8 months of age), the patient was under valganciclovir treatment and CMV replication was controlled. Routine blood test showed normal white blood cell (WBC) and total

lymphocyte counts, increased eosinophil count, mild anemia, and low immunoglobulin levels (Table 1). Lymphoid cells distribution revealed a reduction in CD3⁺ and CD4⁺ percentages, with normal frequency of CD8⁺ and CD3[–]CD16⁺56⁺ NK cells (11.3%) and an expansion of CD19⁺ B cells (41.9%). A reduced frequency of naïve CD4⁺ and CD8⁺ T cells, combined with an expansion of CD45RA[–]CCR7[–] effector memory (47.3%) and CD45RA⁺CCR7[–] terminally differentiated (50.8%) CD8⁺ T cells, was noted (Table 1; Supplementary Fig. S1A), a condition that is coherent with persistent CMV infection.¹⁸ The circulating B-cell fraction showed a marked reduction of total memory B cells CD19⁺CD27⁺ (1.09%) and almost absent switched memory B cells CD27⁺IgD[–]IgM[–] (0.05%) (Table 1; Supplementary Fig. S1B). Such distribution and phenotype of immune cells was maintained at later time points (9 and 11 months of age; data not shown). Finally, by functional tests we observed that T-cell proliferation in response to PHA or OKT3 stimulation was moderately reduced (Table 1), while B-cell response to CpG stimulation was normal in terms of proliferation (data not shown) but impaired as for IgG and IgA secretion (Table 1).

According to the clinical picture and lymphocyte distribution, a leaky SCID was suspected and a de novo hypomorphic c.664C > T; p.R222C mutation of the *IL2RG* gene was finally detected by next generation sequencing (NGS) and confirmed by Sanger sequencing (Fig. 1A,B).

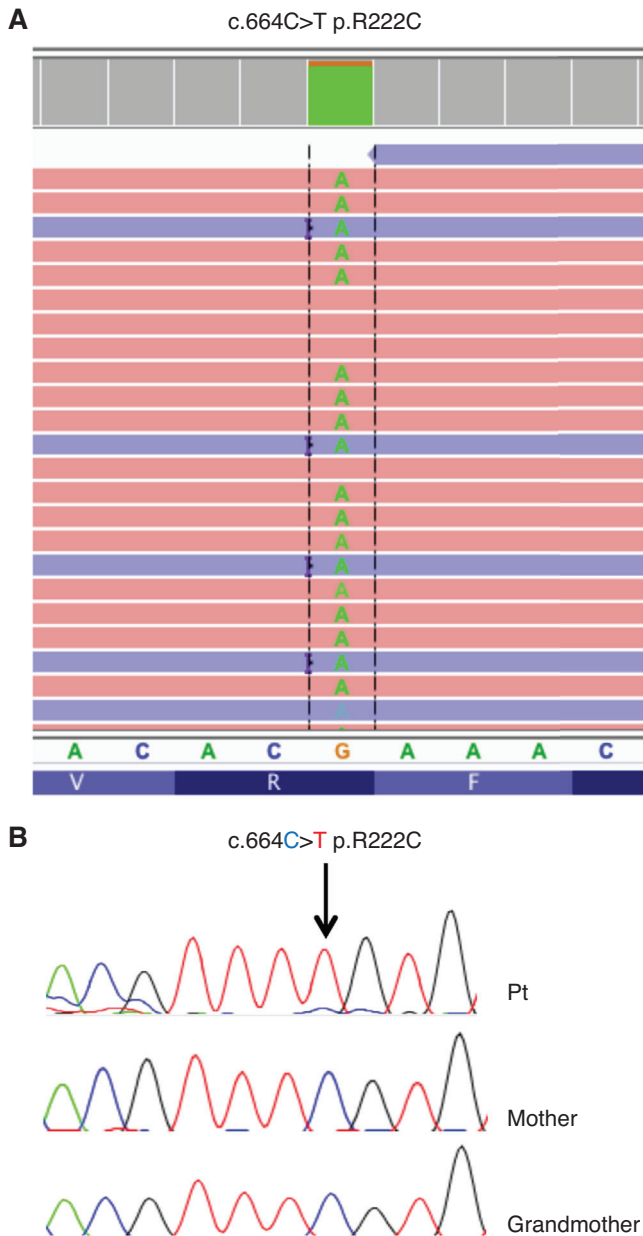


FIGURE 1 Molecular analysis. (A) Sequence alignment of the patient's BAM file on IGV revealed the c.664C > T mutation in the *IL2RG* gene leading to the p.R222C amino-acid change. (B) *IL2RG* Sanger sequence chromatogram in the patient (Pt) and his family members. The mutated residue is indicated (arrow)

In the *IL2RG*^{R222C} patient, the observed reduction of switched memory B cells, which maturation depends on a correct stimulation via CD40L and IL-21,¹⁹ likely resulted from an aberrant B cell-specific γ_c -signaling rather than from an impaired peripheral follicular helper T cells (pTfh) function. Indeed, the frequency of CD4⁺CD45RO⁺CXCR5⁺ pTfh cells that predominantly expressed CXCR3 and PD1 was increased (Table 1; Supplementary Fig. S1C). Apparently, the impaired IL-2 signaling in our patient did not seem to compromise the pTfh cell differentiation, probably because this is not exclusively dependent on γ_c -signaling.^{20,21} The observed PD1⁺ pTfh

cells possibly originated from reprogrammed helper T cells in the context of persistent viral infection (i.e., chronic CMV infection in the *IL2RG*^{R222C} patient), as demonstrated in a mouse model.²² Moreover, in line with previous reports,^{13,14} the *IL2RG*^{R222C} mutation did not result in the complete absence of CD4⁺CD25⁺CD127⁻FOXP3⁺ regulatory T cells (Tregs) in the patient who displayed a reduced overall Treg frequency (Table 1) and a prevalent Treg memory phenotype (Supplementary Fig. S1D).

To determine the capacity of the *IL2RG*^{R222C} mutation to impair the signaling pathway, we evaluated STAT5 phosphorylation. A STAT5 phosphorylation impairment was confirmed on CD4⁺CD45RO⁺ T cells after stimulation with 10U/ml of IL-2, whereas supraphysiological cytokine doses (100 and 1000 U/ml) were able to induce phosphorylation levels comparable to controls (Fig. 2), as previously reported.^{13,14} This result suggested that *IL2RG*^{R222C} allowed T cell development but IL-2 response in memory T cells was functionally impaired, resulting in the atypical immunological picture of the patient. Thus, analysis of STAT5 phosphorylation after stimulation with different concentrations of IL-2 is a rapid functional assay to detect abnormalities in γ_c pathway and it is recommended to make a prompt diagnosis also in cases with atypical presentation.

The NGS alignment on integrative genome viewer (IGV) detected a relevant frequency (10%) of wild-type allele (Fig. 1A). To determine in which cell subset(s), the reverted allele was present, Sanger sequencing of the *IL2RG* gene was performed in purified CD3⁺ T cells, CD19⁺ B cells, NK cells and CD14⁺ monocytes after flow-based sorting of live cell populations. The reverted allele was detected only in 38% of CD3⁺ T cells (Fig. 3A). Then, the analysis was repeated on sorted CD3⁺CD4⁺ subsets, showing that reversion occurred in 30%, 20%, and 56% of RTE, EM, and EMRA cells, respectively (Fig. 3B). Maternal engraftment was ruled out by the analysis of short-tandem repeats.

Patient's NK cells had a normal frequency among PBLs, but their distribution into CD56^{bright}, CD56^{dim}, and CD56^{neg} subsets showed a higher proportion of CD56^{bright} cells (33.1% versus median 15.7% of age-matched healthy donors (HDs); Table 1, Fig. 4A, gating strategy in Supplementary Fig. S2A). The CD56^{bright} NK cells are believed to be precursors of CD56^{dim} cells, release relevant amounts of cytokines upon stimulation, and can play a regulatory function by eliminating autologous activated T cells.²³ The expansion of CD56^{bright} cells has been described in various pathologic settings, such as in HIV-1 infected patients with poor CD4⁺ T cell reconstitution despite suppressive antiretroviral therapy²⁴ and, more recently, in T⁻B⁻NK⁺ SCID patients with mutations in RAG and non-homologous end joining (NHEJ) genes.²⁵ In our patient, we found that expanded CD56^{bright} cells had an immature phenotype (NKG2A⁺NKG2C⁻CD57⁻) (Fig. 4B; Supplementary Fig. S2B), as previously observed in SCID patients with RAG/NHEJ defects.²⁵ By measuring the intracellular perforin level (MFI), we found that, in CD56^{bright} cells, this was 3-fold higher in the *IL2RG*^{R222C} patient as compared with age-matched HDs (22,348 versus 7113 [5667, 8141], median [25th, 75th percentiles] MFI), whereas in patient's CD56^{dim} cells perforin fitted within the highest range of normal expression (37309 vs. 27201 [21533, 32830] MFI). In addition, by measuring expression of the CD107a degranulation marker as a

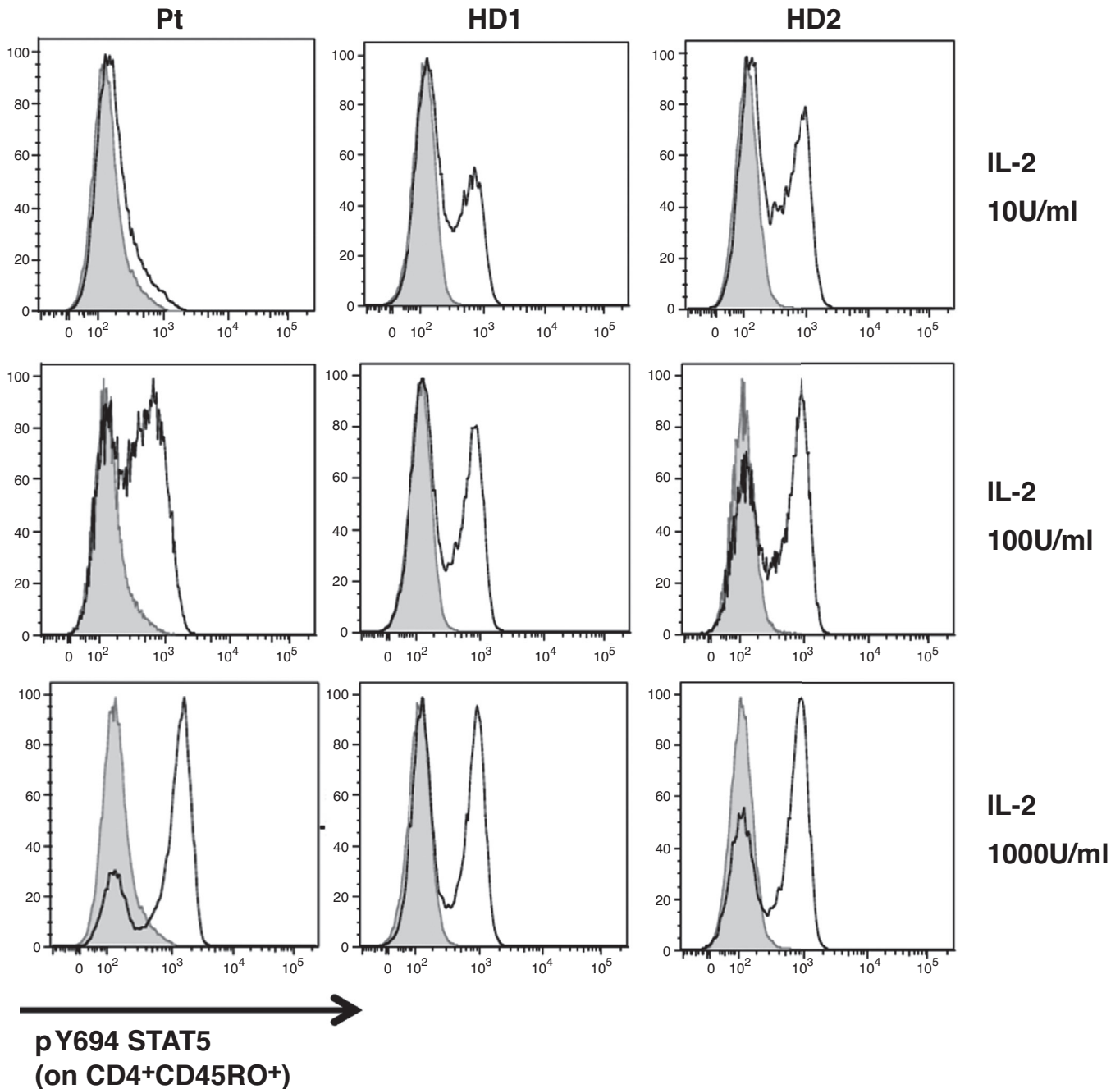


FIGURE 2 Impact of *IL2RG*^{R222C} on STAT5 phosphorylation. The expression of phospho-STAT5 (pY694 STAT5) was analyzed in gated CD4⁺ memory T cells (CD4⁺CD45RO⁺) after incubation of PBMCs in medium alone (shaded area) or supplemented with different IL-2 concentrations (10, 100, and 1000 U/ml) (black lines) in the *IL2RG*^{R222C} patient (Pt) and two healthy donors (HD1, HD2)

direct correlate of NK-cell cytotoxicity, we found that the frequency of CD107a⁺ cells challenged with K562 cells was very high for CD56^{bright} cells of the *IL2RG*^{R222C} patient if compared with age-matched healthy controls, (57.90% versus 26.50 [15.90, 37.10]%), while fell within the normal range for CD56^{dim} cells (10% versus 16.00 [10.60-21.40]%) (Fig. 4D). Therefore, unlike SCID patients with RAG/NHEJ defects,²⁵ CD56^{bright} cells, but not CD56^{dim} cells, displayed higher perforin content and a superior cytotoxic potential in the *IL2RG*^{R222C} patient as compared with HDs. Moreover, patient's NK cells presented normal

ability to produce IFN- γ upon 20 h stimulation with IL-12, IL-15, and IL-18 (Fig. 4E), expressed high levels of the NKG2D activating receptor, and were skewed toward a mature and memory-like phenotype in line with CMV infection (Table 1; Supplementary Fig. S2C and D). The CD56^{dim} memory-like cell subset consists in a highly cytotoxic NK cell population with immune adaptive properties that is found in CMV-seropositive individuals²⁶ and that, together with expanded memory CD8⁺ T cells (Table 1), might have contributed to patient's partial control of CMV replication. Our functional data are

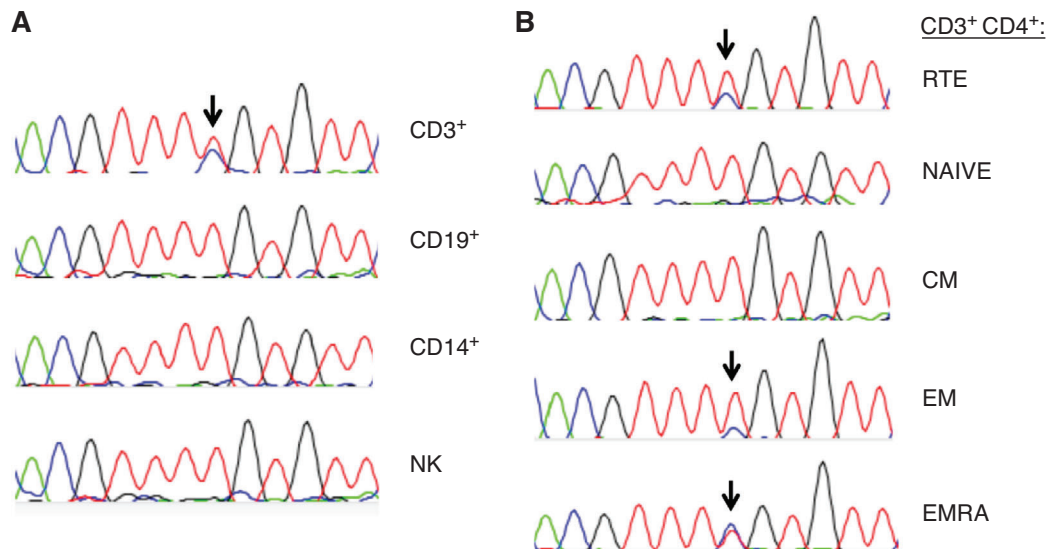


FIGURE 3 Mutation reversion of the *IL2RG* gene in sorted patient's cells. Sanger sequencing of the *IL2RG* gene was performed on sorted cells: (A) CD3⁺ T cells, CD19⁺ B cells, CD14⁺ monocytes, NK cells, and (B) CD4⁺ T recent thymic emigrants (RTE, CD31⁺CD45RA⁺), naïve (CD27⁺CD45RA⁺), central memory (CM, CD27⁺CD45RA⁻), effector memory (EM, CD27⁻CD45RA⁻), and effector memory CD45RA⁺ (EMRA, CD27⁻CD45RA⁺) subpopulations. The mutated residue is indicated (arrow). The experiment was performed twice obtaining the same results

discordant with a previous study on *IL2RG*^{R222C} patients showing defective IFN- γ production by NK cells,¹³ possibly because a different stimulation scheme (5 h of stimulation with IL-15/IL-18) was used. CD56^{bright} cells, which constitutively express both intermediate-affinity ($\beta\gamma_c$) and high-affinity ($\alpha\beta\gamma_c$) IL-2R, are efficiently stimulated by IL-2,²⁷ hence we hypothesized that patient's CD56^{bright} cells expansion could be driven by increased IL-2 availability due to reduced cytokine consumption in the *IL2RG*^{R222C} context. Indeed, we found that IL-2, as well as IL-7 and IL-15, other γ_c cytokines that stimulate NK cells, accumulated in the patient's plasma (Fig. 5). The γ_c cytokines are important factors that regulate the development and functional maturation of NK cells, although the specific role of each cytokine in this process remains unclear.²⁸ It is plausible that, in the *IL2RG*^{R222C} patient, the net balance between defective signaling of γ_c receptors and accumulation of IL-2, IL-7, and IL-15 resulted in the expansion of highly active CD56^{bright} cells while it was not sufficient to promote efficient differentiation and/or survival of CD56^{dim} cells. Moreover, impaired signaling of IL-21, a γ_c cytokine with diverse effects on immune cells, might have influenced the development and functional maturation of NK cells.²⁸ A key role of IL-2 signaling via its high-affinity ($\alpha\beta\gamma_c$) receptor in the homeostasis of NK-cell subsets has been recently underscored by a study on a child with CD25 deficiency caused by a homozygous mutation in the *IL2RA* gene who presented combined immunodeficiency (CID) with recurrent viral and bacterial infections, lymphoproliferations, and severe multi-organs autoimmune disorders.²⁹ Specifically, in this CD25-deficient patient, NK cells had a normal frequency but showed a strong expansion of CD56^{bright} cells (particularly CD56^{bright}CD16⁺ cells) at the expense of CD56^{dim} cells, which were reduced in number and poorly differentiated, and displayed an overall altered NK-cell functionality owing to enhanced perforin expression and cytotoxicity as well as compromised IFN- γ

production.²⁹ Apparently, accumulation of CD56^{bright} cells that have exacerbated perforin expression and cytotoxic responses and do not efficiently proceed through differentiation into CD56^{dim} cells, is a feature shared by CD25 deficiency and *IL2RG*^{R222C} hypomorphism; on the other hand, the *IL2RG*^{R222C} but not the CD25-deficient condition, allowed normal acquisition of IFN- γ production capacity and CD56^{dim} cell maturation and function, possibly mediated by the residual signaling of IL-2 (via both high- and intermediate-affinity IL-2R) and other abundant γ_c cytokines. Altogether, our data indicate that expansion of CD56^{bright} NK cells with a potentially deleterious regulatory function can be found not only in SCID/CID patients with RAG/NHEJ defects²⁵ and CD25 deficiency,²⁹ but also in atypical *IL2RG*^{R222C} patients. Finally, since IL-2 and IL-7 have a key role in Treg cell development and maintenance,³⁰ their increased availability might have supported the differentiation of Treg cells with a mature phenotype that was observed in the *IL2RG*^{R222C} patient (Supplementary Fig. S1D).

Soon after diagnosis, the patient underwent HLA-haploidentical hematopoietic stem cell transplantation (haplo-HSCT) from the mother after negative depletion of T $\alpha\beta^+$ /CD19⁺ lymphocytes (Table 1). The pre-transplant conditioning regimen administered was treosulfan (42 g/m² over 3 days), fludarabine (160 mg/m² for 4 days), and anti T-lymphocyte globulin (ATLG, grafalon, Neovii). On day -1, Rituximab (200 mg/m²) was administered for preventing EBV-related post-transplant lymphoproliferative disorder. The neutrophil and platelet engraftment was reached respectively on day +19 and +34 after transplant.

In previous studies, *IL2RG*^{R222C} patients have been described with normal or only moderately reduced T and NK cell numbers.¹²⁻¹⁴ In these patients, the atypical phenotype makes diagnosis challenging and delayed over time, whereas even neonatal screening could be not indicative. Indeed, *IL2RG*^{R222C} SCID patients are characterized by

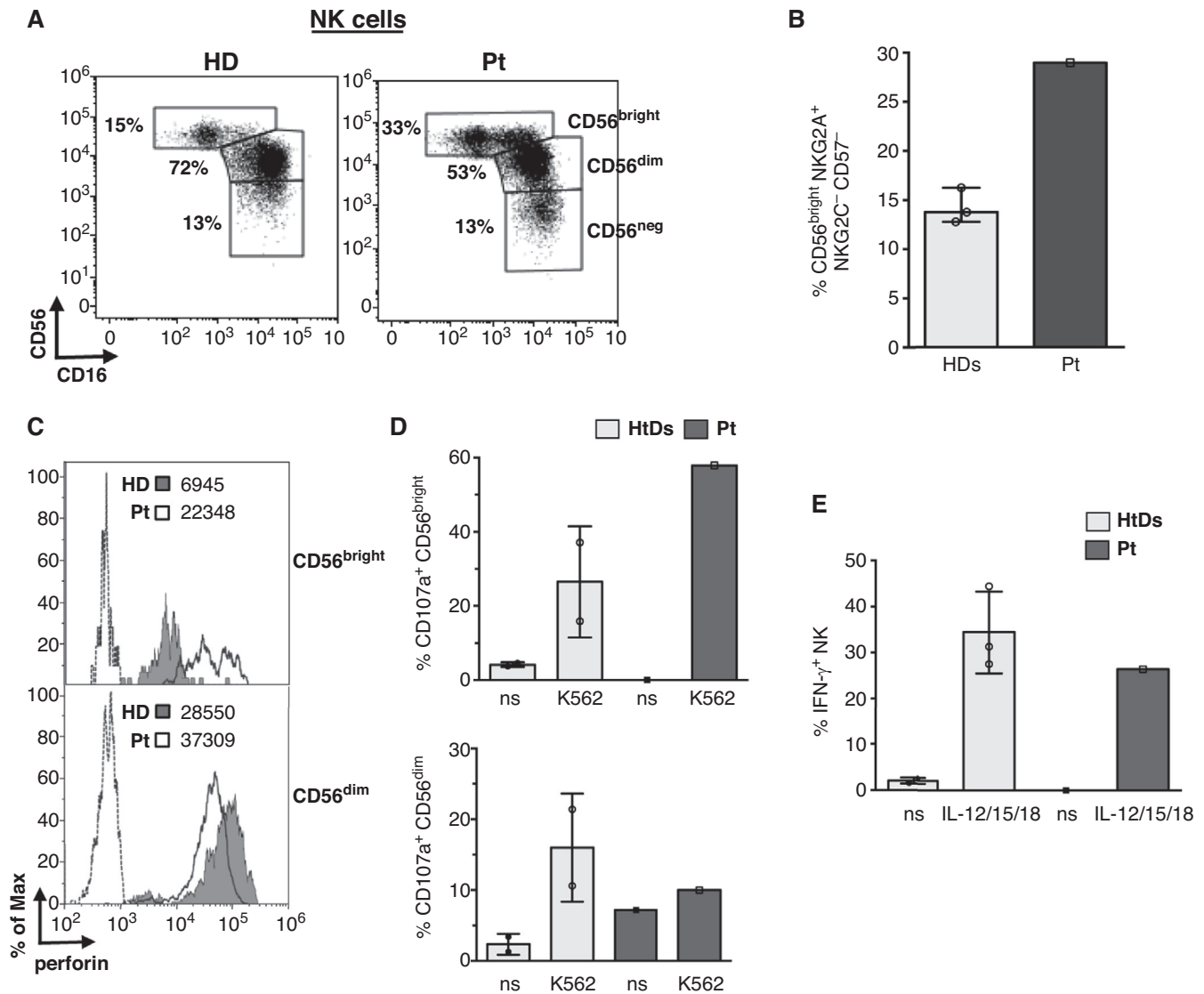


FIGURE 4 CD56^{bright} NK cells with enhanced effector function are expanded in the *IL2RG*^{R222C} patient. (A) NK cells of a representative HD and the *IL2RG*^{R222C} patient (Pt), gated as described in Supplementary Fig. 2A, were analyzed to measure the frequency of CD56^{bright}, CD56^{dim}, and CD56^{neg} subsets. (B) The percentage of CD56^{bright}NKG2A⁺NKG2C⁻CD57⁻ cells among total NK cells was analyzed as described in Supplementary Fig. 2B in the *IL2RG*^{R222C} patient and 3 age-matched HDs (median and range is shown). (C) Histograms show the intracellular perforin expression of gated CD56^{bright} and CD56^{dim} NK cells of the *IL2RG*^{R222C} patient (open histograms) and a representative HD (filled gray histograms). Dashed line represents staining with isotype control IgG. The MFI values are indicated. (D) Bar plots represent pattern of CD107a expression measured by flow cytometry on gated CD56^{bright} and CD56^{dim} NK cells of the *IL2RG*^{R222C} patient and 3 HDs following 6 h culture of PBMCs (effectors, E) with and without (not stimulated, ns) K562 cell targets (T) at an E:T ratio of 10:1. The mean \pm SD of 2 HDs is reported. (E) Bar plots depict percentage of IFN- γ -expressing NK cells from the *IL2RG*^{R222C} patient and 3 HDs (mean \pm SD) analyzed by flow cytometry after 20 h culture of PBMCs in the presence or absence (ns) of IL-12, IL-15, and IL-18

impaired lymphocyte function rather than cell frequency, by reduced but present naïve T cells, and by normal T-cell receptor excision circles (TRECs) that may mislead diagnosis.¹³⁻¹⁴ In this context, functional studies dissecting activation markers after cytokine stimulation may facilitate the diagnosis of hypomorphic *IL2RG* mutation and direct faster molecular analyses.

Our report further informs on phenotypic and functional alterations of the NK-cell compartment to be investigated in the suspicion of X-SCID with hypomorphic *IL2RG* mutation.

AUTHORSHIP

C.C.F., N.C., and M.D. wrote the manuscript. C.C.F., S.D.C., N.C., and M.D. performed experiments. C.C.F., N.C., M.D., and C.C., discussed and interpreted the results. P.R., F.L., A.F., N.C., P.Z., D.A., D.B., D.P., and S.G. provided clinical samples and patient's clinical data. G.S. performed NGS. C.C., A.F., and M.D. provided funding. C.C., S.D.C., G.D.M., C.M., and A.F. participated to the study design and data interpretation. C.C. and M.D. supervised the research and manuscript revision. All authors provided scientific input and

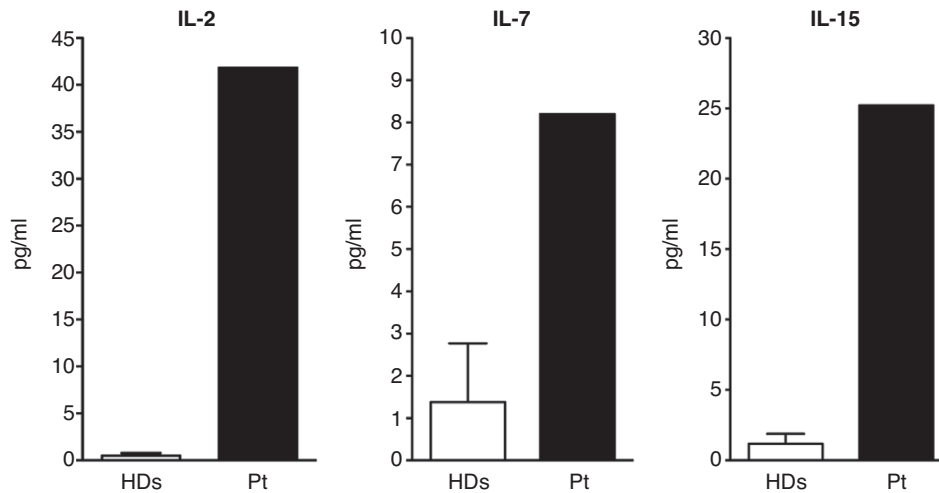


FIGURE 5 High IL-2, IL-7, and IL-15 concentration in patient's plasma. Cytokine profiles in the *IL2RG*^{R222C} patient and healthy subjects. Plasma concentration of IL-2, IL-7, and IL-15 was determined for the *IL2RG*^{R222C} patient and 4 age-matched HDs using a multiplex method. Values represent average of duplicates. Bars indicate mean \pm SD

revised the final version of the manuscript. (CCF, Cristina Cifaldi; CC, Caterina Cancrini). C.C.F. and N.C. have contributed equally to this work. C.C. and M.D. share last authorship. C.C. and N.C. contributed equally to this work. M.D. and C.C. are Joint First Authors.

ACKNOWLEDGMENTS

We acknowledge the parents of the patient, nurses, and colleagues at the Immune and Infectious Disease unit at the University Department of Pediatrics, Bambino Gesù Children's Hospital. The study was supported by grants of the Italian Ministry of Health to CC (NET-2011-02350069), Ricerca Corrente from Bambino Gesù Children's Hospital, Rome, Italy to C.C. and M.D., and by Fondazione Telethon grant to A.F. (GGP15109).

DISCLOSURE

The authors declare no conflict of interest.

ORCID

Margherita Doria  <https://orcid.org/0000-0001-5533-0304>

REFERENCES

- Kovanen PE, Leonard WJ. Cytokines and immunodeficiency diseases: critical roles of the gamma(c)-dependent cytokines interleukins 2, 4, 7, 9, 15, and 21, and their signaling pathways. *Immunol Rev*. 2004;202:67-83.
- Klatzmann D, Abbas AK. The promise of low-dose interleukin-2 therapy for autoimmune and inflammatory diseases. *Nat Rev Immunol*. 2015;15:283-294.
- Rochman Y, Spolski R, Leonard WJ. New insights into the regulation of T cells by gamma(c) family cytokines. *Nat Rev Immunol*. 2009;9:480-490.
- Sugamura K, Asao H, Kondo M, et al. The interleukin-2 receptor gamma chain: its role in the multiple cytokine receptor complexes and T cell development in XSCID. *Annu Rev Immunol*. 1996;14:179-205.
- Noguchi M, Yi H, Rosenblatt HM, et al. Pillars article: interleukin-2 receptor gamma chain mutation results in X-linked severe combined immunodeficiency in humans. *Cell*. 1993;73:147-157. *J Immunol*. 1993;181:5817-5827.
- Fischer A, Notarangelo LD, Neven B, Cavazzana M, Puck JM. Severe combined immunodeficiencies and related disorders. *Nat Rev Dis Primers*. 2015;1:15061.
- Notarangelo LD. Primary immunodeficiencies. *J Allergy Clin Immunol*. 2010;125:S182-S194.
- Brown L, Xu-Bayford J, Allwood Z, et al. Neonatal diagnosis of severe combined immunodeficiency leads to significantly improved survival outcome: the case for newborn screening. *Blood*. 2011;117:3243-3246.
- Hacein-Bey-Abina S, Pai SY, Gaspar HB, et al. A modified gamma-retrovirus vector for X-linked severe combined immunodeficiency. *N Engl J Med*. 2014;371(15):1407-1417.
- De Ravin SS, Wu X, Moir S, et al, Kardava, et al. Lentiviral hematopoietic stem cell gene therapy for X-linked severe combined immunodeficiency. *Sci Transl Med*. 2016;8(335):335ra357.
- Cifaldi C, Ferrua F, Aiuti A, Cancrini C. Hematopoietic stem cell gene therapy for the cure of blood diseases: primary immunodeficiencies. *Rend Fis Acc Lincei*. 2018;29:755.
- Sharfe N, Shahar M, Roifman CM. An interleukin-2 receptor gamma chain mutation with normal thymus morphology. *J Clin Invest*. 1997;100:3036-3043.
- Fuchs S, Rensing-Ehl A, Erlacher M, et al. Patients with T(+)/low NK(+) IL-2 receptor gamma chain deficiency have differentially-impaired cytokine signaling resulting in severe combined immunodeficiency. *Eur J Immunol*. 2014;44:3129-3140.
- Stepensky P, Keller B, Shamriz O, et al. T(+) NK(+) IL-2 receptor gamma chain mutation: a challenging diagnosis of atypical severe combined immunodeficiency. *J Clin Immunol*. 2018;38:527-536.
- Stephan V, Wahn V, Le Deist F, et al. Atypical X-linked severe combined immunodeficiency due to possible spontaneous reversion of the genetic defect in T cells. *N Engl J Med*. 1996;335:1563-1567.
- Kuijpers TW, van Leeuwen EM, Barendregt BH, et al. A reversion of an IL2RG mutation in combined immunodeficiency providing competitive advantage to the majority of CD8+ T cells. *Haematologica*. 2013;98:1030-1038.
- Cifaldi C, Brigida I, Barzaghi F, et al. Targeted NGS platforms for genetic screening and gene discovery in primary immunodeficiencies. *Front Immunol*. 2019;10:316.

18. Klenerman P, Oxenius A. T cell responses to cytomegalovirus. *Nat Rev Immunol.* 2016;16:367-377.
19. Recher M, Berglund LJ, Avery DT, et al. IL-21 is the primary common γ chain-binding cytokine required for human B-cell differentiation in vivo. *Blood.* 2011;118(26):6824-6835.
20. Tangye SG, Ma CS, Brink R, Deenick EK. The good, the bad and the ugly—TFH cells in human health and disease. *Nat Rev Immunol.* 2013;13(6):412-426.
21. Read KA, Powell MD, Oestreich KJ. T follicular helper cell programming by cytokine-mediated events. *Immunology.* 2016;149(3):253-261.
22. Fahey LM, Wilson EB, Elsaesser H, Fistonich CD, McGavern DB, Brooks DG. Viral persistence redirects CD4 T cell differentiation toward T follicular helper cells. *J Exp Med.* 2011;208(5):987-999.
23. Michel T, Poli A, Cuapio A, et al. Human CD56^{bright} NK cells: an update. *J Immunol.* 2016;196(7):2923-2931. <https://doi.org/10.4049/jimmunol.1502570>.
24. Giuliani E, Vassena L, Di Cesare S, et al. NK cells of HIV-1-infected patients with poor CD4(+) T-cell reconstitution despite suppressive HAART show reduced IFN- γ production and high frequency of autoreactive CD56^{bright} cells. *Immunol Lett.* 2017;190:185-193.
25. Dobbs K, Tabellini G, Calzoni E, et al. Corrigendum: natural killer cells from patients with recombinase-activating gene and non-homologous end joining gene defects comprise a higher frequency of CD56^{bright} NKG2A⁺⁺⁺ cells, and yet display increased degranulation and higher perforin content. *Front Immunol.* 2017;8:1244.
26. Della Chiesa M, De Maria A, Muccio L, Bozzano F, Sivori S, Moretta L. Human NK cells and herpesviruses: mechanisms of recognition, response and adaptation. *Front Microbiol.* 2019;10:2297.
27. Caligiuri MA, Zmuidzinas A, Manley TJ, Levine H, Smith KA, Ritz J. Functional consequences of interleukin 2 receptor expression on resting human lymphocytes. Identification of a novel natural killer cell subset with high affinity receptors. *J Exp Med.* 1990;171:1509-1526.
28. Wu Y, Tian Z, Wei H. Developmental and functional control of natural killer cells by cytokines. *Front Immunol.* 2017;8:930.
29. Caldirola MS, Rodríguez Broggi MG, Gaillard MI, Bezrodnik L, Zwirner NW. Primary immunodeficiencies unravel the role of IL-2/CD25/STAT5b in human natural killer cell maturation. *Front Immunol.* 2018;9:1429.
30. Fan MY, Low JS, Tanimine N, et al. Differential roles of IL-2 signaling in developing versus mature Tregs. *Cell Rep.* 2018;25(5):1204-1213.e4. <https://doi.org/10.1016/j.celrep.2018.10.002>.
31. Schatorje EJ, Gemen EF, Driessen GJ, Leuvenink J, van Hout RW, de Vries E. Paediatric reference values for the peripheral T cell compartment. *Scand J Immunol.* 2012;75(4):436-444.
32. Duchamp M, Sterlin D, Diabate A, et al. B-cell subpopulations in children: national reference values. *Immun Inflamm Dis.* 2014;2(3):131-140.
33. Schatorje EJ, Gemen EF, Driessen GJ, et al. Age-matched reference values for B-lymphocyte subpopulations and CVID classifications in children. *Scand J Immunol.* 2011;74(5):502-510.
34. Marasco E, Farroni C, Cascioli S, et al. B-cell activation with CD40L or CpG measures the function of B-cell subsets and identifies specific defects in immunodeficient patients. *Eur J Immunol.* 2017;47(1):131-143.

SUPPORTING INFORMATION

Additional information may be found online in the Supporting Information section at the end of the article.

How to cite this article: Cifaldi C, Cotugno N, Di Cesare S, et al. Partial T cell defects and expanded CD56^{bright} NK cells in an SCID patient carrying hypomorphic mutation in the *IL2RG* gene. *J Leukoc Biol.* 2020;108:739–748. <https://doi.org/10.1002/JLB.5MA0220-239R>